Low energy strength in low-multipole response function of nuclei near the neutron drip line

I. Hamamoto[1] and H. Sagawa[2]
[1]Department of Mathematical Physics, Lund Institute of Technology at University of Lund, Lund, Sweden
[2]Center for Mathematical Sciences, University of Aizu, Ikki-machi, Aizu-Wakamatsu, Fukushima 965, Japan
(Received 21 December 1995)

The very low-energy transition strength unique in neutron drip line nuclei is studied, taking an example of ${}^{28}_{8}\mathrm{O}_{20}$ and performing the Hartree-Fock plus RPA calculation with Skyrme interaction. The most dramatic example is monopole modes, however, an appreciable amount of isovector dipole strength may appear also in the very low excitation energy. Unperturbed response functions are carefully studied, which contain all basic information on the exotic behavior of the RPA strength function. The low-energy transition strength is induced by the excitations of neutrons, which have smaller binding energies and smaller angular momenta. The neutrons with a few MeV binding energies are sufficient for obtaining this strength, and the phenomena are differentiated from the so-called soft multipole excitations in halo nuclei.

PACS number(s): 21.10.Pc, 21.10.Re, 21.60.Jz, 27.30.+t

Various new exotic properties are expected for nuclei far from β stability, which can be reached using radioactive nuclear beams [1]. Among others, collective properties of neutron drip line nuclei are especially interesting [2], because neutrons with small binding energies show a unique response to external fields in contrast to protons with small binding energies, which behave differently due to the presence of the Coulomb barrier. However, in medium-heavy nuclei the neutron drip line will not be experimentally reached in the near future. In very light nuclei along the neutron drip line, such as ${}^{11}_{3}\mathrm{Li}_{8}$, ${}^{11}_{4}\mathrm{Be}_{7}$, and ${}^{14}_{4}\mathrm{Be}_{10}$, exotic halo phenomena are found and studied [3–5], which come from the presence of neutrons with extremely small binding energies ($\lesssim$0.5 MeV) and small orbital angular momenta ($\ell=0$ or 1). In this Rapid Communication we examine the response function of light neutron drip line nuclei, which do not show halo phenomena. Taking the nuclei ${}^{28}_{8}\mathrm{O}_{20}$ as a numerical example we analyze the single-particle response function for each occupied orbit, which provides the basis for the understanding of the response function obtained in the random-phase approximation (RPA).

The model is the same as the one used in [2]. First, we perform the spherical Hartree-Fock (HF) calculation with Skyrme interactions. Being interested in monopole response functions we choose the SkM* interaction among Skyrme interactions, since it has a favored value (namely, 216 MeV) of the incompressibility for the nuclear matter. We estimate collective properties solving the RPA with the Green's function method in the coordinate space, which produces a proper strength function in the continuum [6,7], though the spreading width of collective modes is not included. Characteristic features of the exotic response function obtained from the RPA [2] can be understood by a careful examination of the unperturbed strength function.

We examine both the unperturbed strength function

$$S_0(E)\equiv\sum_i |\langle i|Q|0\rangle|^2\delta(E-E_i)$$
$$=\frac{1}{\pi}\,\mathrm{Im}\,\mathrm{Tr}[Q^\dagger G_0(E)Q], \tag{1}$$

where G_0 is the noninteracting particle-hole (p-h) Green function and the RPA strength function

$$S(E)\equiv\sum_n |\langle n|Q|0\rangle|^2\delta(E-E_n)$$
$$=\frac{1}{\pi}\,\mathrm{Im}\,\mathrm{Tr}(Q^\dagger G_{\mathrm{RPA}}(E)Q). \tag{2}$$

In Eqs. (1) and (2) Q expresses one-body operators, which are written as

$$Q^{\lambda=0,\tau=0}=\sum_i r_i^2 Y_{00}(\hat{r}_i)$$

for isoscalar monopole modes, (3)

$$Q^{\lambda=0,\tau=1}=\sum_i \tau_z r_i^2 Y_{00}(\hat{r}_i)$$

for isovector monopole modes, and (4)

$$Q_\mu^{\lambda=1,\tau=1}=\sum_i \tau_z r_i Y_{1\mu}(\hat{r}_i)$$

for isovector dipole modes. (5)

The unperturbed strength function defined in Eq. (1) does not contain the strength of the bound p-h excitations, in which the particle is excited from a bound hole orbital to a bound particle orbital. In the case of ${}^{28}_{8}\mathrm{O}_{20}$ there are no such bound p-h excitations of neutrons for any multipoles, while for protons the main monopole as well as dipole strength comes from the bound p-h excitations and, thus, is not included in expression (1). However, since the energies of those p-h excitations are above the particle threshold (1.79 MeV, which is the neutron threshold in ${}^{28}_{8}\mathrm{O}_{20}$), the strength of those p-h excitations appears in the calculated RPA strength function in (2), due to the coupling to the continuum.

TABLE I. One-particle properties of ${}^{28}_{8}O_{20}$ in the Hartree-Fock calculation with the SkM* interaction. The HF single-particle energies ϵ are listed together with the expectation values of r^2 and r^4 for each orbit. For some single-particle orbitals lying in the continuum the estimated single-particle resonance energies are given. See the text for details.

1. Protons											
Orbitals	$1s_{1/2}$	$1p_{3/2}$	$1p_{1/2}$	$1d_{5/2}$	$2s_{1/2}$	$1d_{3/2}$	$1f_{7/2}$	$2p_{3/2}$	$2p_{1/2}$	$(1f_{5/2})_{\rm res}$	$(1g_{9/2})_{\rm res}$
ϵ (MeV)	−44.1	−31.69	−27.02	−19.35	−15.11	−12.37	−6.63	−2.36	−0.70	+0.64	+5.68
$\langle r^2\rangle$ (fm^2)	5.43	8.79	9.07	11.73	12.26	13.17	15.09	21.73	26.99		
$\langle r^4\rangle$ (fm^4)	47.64	104.4	113.0	174.9	236.8	225.1	288.7	775.0	1305.5		
2. Neutrons											
Orbitals	$1s_{1/2}$	$1p_{3/2}$	$1p_{1/2}$	$1d_{5/2}$	$2s_{1/2}$	$1d_{3/2}$	$(1f_{7/2})_{\rm res}$	$(2p_{3/2})_{\rm res}$	$(2p_{1/2})_{\rm res}$	$(1f_{5/2})_{\rm res}$	$(1g_{9/2})_{\rm res}$
ϵ (MeV)	−31.94	−19.93	−14.94	−8.64	−5.99	−1.79	+1.59			(+9.9)	(+12.0)
$\langle r^2\rangle$ (fm^2)	5.09	8.70	9.20	12.96	16.69	18.22					
$\langle r^4\rangle$ (fm^4)	43.00	107.9	124.4	229.4	449.8	552.6					

In Table I we show HF single-particle energies and expectation values of r^2 and r^4. Unoccupied single-particle levels are estimated for the calculated HF potential. For some levels lying in the continuum, which we are interested in, estimated single-particle resonance energies are given. The resonant states are found so that the phase shift passes through $\pi/2$ with positive slope at the single-particle energies. In the case of neutrons we could not obtain resonant states for $2p_{3/2}$ and $2p_{1/2}$ orbitals. Furthermore, though the phase shift of the $1f_{5/2}$ and $1g_{9/2}$ orbitals passes through $\pi/2$ at the energy given in Table I the related width is found to be in the order of the resonance energies. Thus, the latter two ''single-particle resonances'' are practically meaningless, and the $1f_{7/2}$ resonance is the only single-particle resonant state which plays an important role in the response function.

In Fig. 1(a) we show the unperturbed strength function in Eq. (1) and the RPA strength function in Eq. (2) for the isoscalar and the isovector monopole modes. The dotted line in Fig. 1(a) happens to contain the neutron strength only and, indeed, includes the whole neutron strength in the plotted energy region. The proton bound p-h excitations for monopole lie at 26.32, 29.00, and 29.33 MeV for $1p_{1/2}\rightarrow 2p_{1/2}$, $1s_{1/2}\rightarrow 2s_{1/2}$, and $1p_{3/2}\rightarrow 2p_{3/2}$, respectively, which do not appear in the dotted line. However, the presence of those bound p-h excitations can be clearly seen in the RPA strength function, which are denoted by the solid and the dashed line for the isoscalar and the isovector mode, respectively.

In Fig. 1(a) it is seen that neither the isoscalar nor the isovector RPA strength is concentrated in a narrow energy region around, say, $65A^{-1/3}=21.4$ MeV or $170A^{-1/3}=56.0$ MeV estimated in a hydrodynamical model [9]. In particular, a considerable strength appears in a surprisingly low-energy region. Since the characteristic feature of the monopole modes in neutron drip line nuclei is already discussed in [2], here we do not repeat it again. However, it is clear that the strength appearing in the very low-energy region is induced by the neutron unperturbed strength in the same energy region. Thus, in the following we analyze the unperturbed monopole strength.

In Fig. 1(b) we resolve the strength expressed by the dotted line in Fig. 1(a) into the strengths, each of which comes from a definite neutron orbital occupied in the ground state. The sum of all strengths in Fig. 1(b) at a given energy is equal to the unperturbed strength in Fig. 1(a) at the same energy. Since the binding energies ($\equiv\epsilon_B$) of $1d_{3/2}, 2s_{1/2}, 1d_{5/2}, \ldots,$ orbitals are 1.79, 5.99, 8.64, . . . , MeV, the corresponding strength starts to appear at respective energies. Using a general argument, it is known [8] that just above the threshold the strength for neutrons rises as the $\ell+1/2$ power of the available energy, namely, as $(E-\epsilon_B)^{\ell+1/2}$. Indeed, in Fig. 1(b) it is seen that the strength with $(1d_{3/2})^{-1}$ and $(1s_{1/2})^{-1}$ rises as $(E-\epsilon_B)^{5/2}$ and $(E-\epsilon_B)^{1/2}$, respectively, since for the monopole mode the orbital angular momentum of the particle must be the same as that of the hole. The monopole strength with a hole in the $1d_{3/2}$ orbital, for example, reaches the maximum around the excitation energy of 4.65 MeV, which is extremely small compared with the harmonic oscillator estimate $2\hbar\omega_0\simeq 27$ MeV, and has a large tail on the high energy side. We note that none of the particle orbitals of the p-h configurations in Fig. 1(b), namely $2d_{3/2}$, $3s_{1/2}$, $2d_{5/2}$, $2p_{1/2}$, and $2p_{3/2}$, appear as resonant states.

Not only the fact that the strength starts to appear at a low energy but also the fact that the average excitation energy of the strength is so low is the consequence of the small binding energies of neutrons. Assuming that the matrix elements of r^2 between the orbitals with a given j and $\Delta n\geqslant 2$ are negligibly small, one might estimate the average energy of the monopole excitation of particles in the (n,j) orbital using the formula

$$E_{\rm av}(n,j)=S1(j)/S0(n,j), \qquad (6)$$

where n denotes the radial node, while all orbitals with a given j and $n'\leqslant n$ are occupied in the ground state. The quantities in Eq. (6), $S1(j)$ and $S0(n,j)$, are written as

$$S1(j)=\frac{2\hbar^2}{m}\sum_{n'\leqslant n}(2j+1)\langle n'j|r^2|n'j\rangle, \qquad (7)$$

$$S0(n,j)=(2j+1)|\langle nj|r^2|n+1,\ j\rangle|^2, \qquad (8)$$

where the sum of $S1(j)$ over j is equal to the energy weighted sum rule

$$S_{\mathrm{EW}}^{\lambda=0}=\sum_{j} S1(j)=\frac{2\hbar^2}{m}A\langle r^2\rangle. \quad (9)$$

In the case of $^{28}_{8}O_{20}$ we can write, for example,

$$E_{\mathrm{av}}(1d_{3/2})=\frac{2\hbar^2}{m}\frac{\langle 1d_{3/2}|r^2|1d_{3/2}\rangle}{\langle 1d_{3/2}|r^4|1d_{3/2}\rangle-|\langle 1d_{3/2}|r^2|1d_{3/2}\rangle|^2} \quad (10)$$

and

$$E_{\mathrm{av}}(2s_{1/2})=\frac{2\hbar^2}{m}\frac{\langle 2s_{1/2}|r^2|2s_{1/2}\rangle+\langle 1s_{1/2}|r^2|1s_{1/2}\rangle}{\langle 2s_{1/2}|r^4|2s_{1/2}\rangle-(|\langle 2s_{1/2}|r^2|2s_{1/2}\rangle|^2+|\langle 2s_{1/2}|r^2|1s_{1/2}\rangle|^2)}. \quad (11)$$

The formula (6) gives the peak energy if the whole strength is concentrated into one sharp peak. In the harmonic oscillator model we obtain $E_{\mathrm{av}}(n,j)=2\hbar\omega_0$ irrespective of (n,j) values. Since the strength functions shown in Fig. 1(b) have a large tail on the high-energy side of respective peaks, formula (6) gives an energy larger than the peak energy; we obtain $E_{\mathrm{av}}(1d_{3/2})=6.9$ MeV and $E_{\mathrm{av}}(2s_{1/2})=11.6$ MeV. Nevertheless, $E_{\mathrm{av}}(n,j)$ in (6) gives a semiquantitative estimate of the energy region where the major part of the strength is found.

The small average energies of the monopole excitation of neutrons in neutron drip line nuclei can be understood in the following way. If we take an example of $n=1$ orbitals such as $1d_{3/2}$ in (10), E_{av} is inversely proportional to $\langle r^2\rangle[(\langle r^4\rangle/\langle r^2\rangle^2)-1]$. The factor $(\langle r^4\rangle/\langle r^2\rangle^2)-1$ is systematically larger for smaller ℓ values, and increases as particle binding energies decrease. Furthermore, the factor $\langle r^2\rangle$ is larger for orbitals with smaller binding energies. Thus, we find that $E_{\mathrm{av}}(n,j)$ is smaller for particles in the (n,j) orbital with smaller binding energies and smaller ℓ values. We obtain similar findings also for orbitals with $n>1$ such as $2s_{1/2}$ in (11), using a similar argument.

Expression (6) is meaningful also for the case in which the particle orbital $(n+1,\ j)$ appears as a resonant state. However, in the case that the $(n+1,\ j)$ orbital can be a one-particle resonant state with a reasonably narrow width, the (n,j) orbital is necessarily a deeply bound state. Therefore, the value of $E_{\mathrm{av}}(n,j)$ would not be far away from $2\hbar\omega_0$ expected from the harmonic oscillator model.

In Fig. 2(a) we show the unperturbed strength function in Eq. (1) and the RPA strength function in Eq. (2) for the isovector dipole mode. As in the case of monopole modes, the dotted line contains the neutron strength only and includes the whole neutron strength in the plotted energy region. The bound p-h excitations of protons lie at 11.91, 12.34, 14.65, 16.58, and 19.32 MeV for $1p_{1/2}\rightarrow 2s_{1/2}$, $1p_{3/2}\rightarrow 1d_{5/2}$, $1p_{1/2}\rightarrow 1d_{3/2}$, $1p_{3/2}\rightarrow 2s_{1/2}$, and $1p_{3/2}\rightarrow 1d_{3/2}$, respectively, which do not appear in the dotted line. However, their presence can be seen in the RPA strength function denoted by the solid line. The RPA isovector dipole strength is seen to spread over a very wide energy region. In particular, an appreciable strength starts to appear already just above 2 MeV. It is clear that the RPA strength in the very low-energy region comes from the neutron unperturbed strength in the same energy region. Thus, we analyze the unperturbed dipole strength.

In Fig. 2(b) the unperturbed strength expressed by the dotted line in Fig. 2(a) is resolved into the components, each of which comes from a definite neutron orbital occupied in the ground state. The strength with the $(1d_{3/2})^{-1}$ configuration, which is denoted by the solid line in Fig. 2(b), starts to appear at 1.79 MeV and contains, roughly speaking, two peaks around 2.6 and 8.1 MeV. The lower peak comes from the $\ell=1$ particles, while the higher one from the $\ell=3$ particles. The strength with the $(1d_{5/2})^{-1}$ configuration starts to appear at 8.64 MeV and contains two peaks at 9.2 and 10.23 MeV. The lower one is connected with $\ell=1$ particles, while the sharp peak at 10.23 MeV comes from the transition of particles from the $1d_{5/2}$ orbital at -8.64 MeV to the $1f_{7/2}$ one-particle resonant state at $+1.59$ MeV. The latter is the only unperturbed dipole excitation, in which a well-defined one-particle resonant state is available. Figure 2(b) illustrates the situation that if a well-defined one-particle resonant state is available the corresponding response strength appears as a sharp peak at the expected energy and, if not, the major transition strength coming from neutrons with small binding energies may shift to the low-energy region. In the latter case the average excitation energy of the dipole strength is lower for neutron holes with smaller binding energies as well as smaller ℓ values.

In the case of β-stable (closed shell as well as open shell) nuclei the major part of both the monopole strength and the dipole strength appears as giant resonances at high energies [9]. In β-stable open-shell nuclei the low-energy quadrupole strength has been systematically observed, which may have quite a different structure from the low-energy strength in neutron drip line nuclei [2]. The former appears usually in discrete states with collective quadrupole nature, which consists mainly of $\Delta N=0$ excitations collecting the strength also from the coupling to $\Delta N=2$ excitations. In contrast, the latter low-energy quadrupole strength is due to the same mechanism as studied here for lower multipoles and lies in the continuum. And, the transition densities have the radial dependence unique in the threshold strength, which is quite different from the surface-peaked form factor of the low-energy collective quadrupole transitions in β-stable nuclei.

In conclusion, taking $^{28}_{8}O_{20}$ as a numerical example, we analyzed the appearance of the very low-energy RPA transition strength unique in neutron drip line nuclei, in terms of unperturbed response functions. The low-energy transition strength will appear in the nuclei, in which the neutrons with

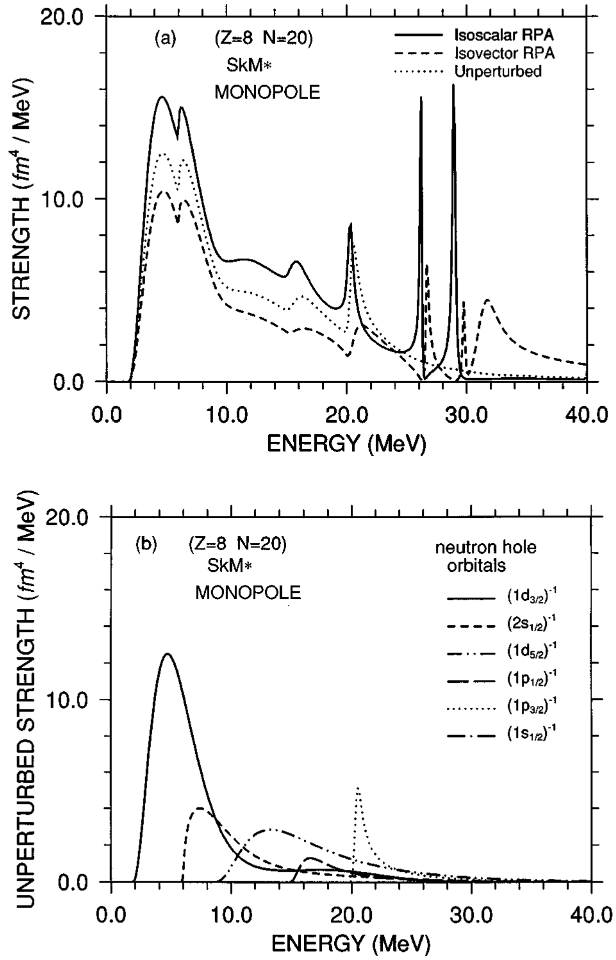

FIG. 1. (a) The unperturbed strength function defined in Eq. (1) and the RPA strength function in Eq. (2) for the isoscalar and the isovector monopole mode of ${}^{28}_{8}O_{20}$ as a function of excitation energy. The unperturbed strength function is the same for the isoscalar and the isovector operator. At 26.32, 29.00, and 29.33 MeV the bound proton p-h excitations are present, which do not appear in the dotted line. However, the presence of those p-h excitations can be recognized as peaks seen in the RPA strength function. See the text for details. (b) Resolving the unperturbed strength in (a) into the components with a given orbital of neutron holes. The strength with the $1s_{1/2}$ hole orbital is so weak that it is not recognizable in the figure. The sum of all strength at a given energy in the figure is equal to the unperturbed strength in (a) at the same energy.

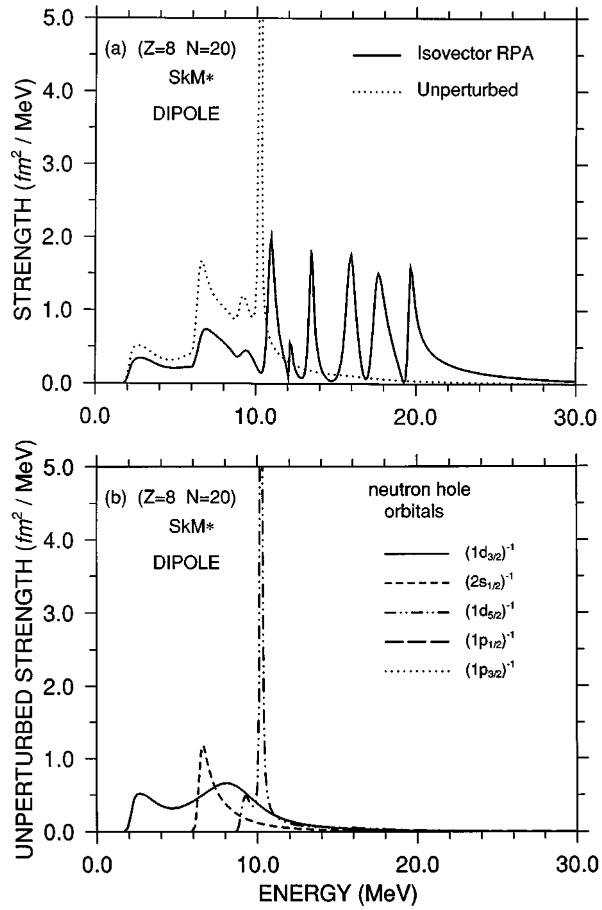

FIG. 2. (a) The unperturbed strength function defined in Eq. (1) and the RPA strength function in Eq. (2) for the isovector dipole mode of ${}^{28}_{8}O_{20}$ as a function of excitation energy. In the region of 11.9–19.3 MeV several bound proton p-h excitations are present, which do not appear in the dotted line. However, the RPA solution contains all strength. See the text for details. (b) Resolving the unperturbed strength in (a) into the components with a given orbital of neutron holes. The strength with the $1p_{1/2}$ and the $1p_{3/2}$ hole orbitals is so weak that it is not visible in the figure. The sum of all strength at a given energy in the figure is equal to the unperturbed strength in (a) at the same energy.

smaller binding energies and smaller angular momenta are present in the ground state. The appearance of the low-energy strength is differentiated from the so-called soft multipole excitations in halo nuclei, to which only the halo neutrons have an essential contribution. The most dramatic example is the monopole modes, however, we expect that an appreciable amount of isovector dipole strength would appear also at very low excitation energies. This low-enegy dipole strength may be feasible for being observed in future experiments.

[1] For example, see, C. Detraz and D. C. Vieira, Annu. Rev. Nucl. Part. Sci. **39**, 407 (1989); I. Tanihata, *Treatise on Heavy-Ion Science*, edited by D. A. Bromley (Plenum, New York and London, 1989), Vol. 8, pp. 443–514; E. Roeckl, Rep. Prog. Phys. **55**, 1661 (1992); A. C. Mueller and B. M. Sherrill, Annu. Rev. Nucl. Part. Sci. **43**, 529 (1993).

[2] I. Hamamoto, H. Sagawa, and X. Z. Zhang, Phys. Rev. C **53**, 765 (1996).

[3] I. Tanihata, H. Hamagaki, O. Hashimoto, Y. Shida, N. Yoshikawa, K. Sugimoto, O. Yamakawa, T. Kobayashi, and Y. Takahashi, Phys. Rev. Lett. **55**, 2676 (1985); P. G. Hansen and B. Jonson, Europhys. Lett. **4**, 409 (1987).

[4] For the experimental information on soft multipole excitations in halo nuclei see, K. Ieki *et al.*, Phys. Rev. Lett. **70**, 730 (1993); T. Nakamura *et al.*, Phys. Lett. B **331**, 296 (1994).
[5] For calculations of soft multipole excitations in halo nuclei, see, H. Sagawa, Nucl. Phys. **A538**, 619c (1992); H. Sagawa, N. Van Giai, N. Takigawa, M. Ishihara, and K. Yazaki, Z. Phys. A **351**, 385 (1995).
[6] S. Shlomo and G. Bertsch, Nucl. Phys. **A243**, 507 (1975).
[7] N. Van Giai and H. Sagawa, Nucl. Phys. **A371**, 1 (1981).
[8] J. M. Blatt and V. F. Weisskopf, *Theoretical Nuclear Physics* (Wiley, New York, 1952), Chap. VIII.
[9] A. Bohr and B. R. Mottelson, *Nuclear Structure*, Vol. II, Sect. 6A-3 (Benjamin, Reading, Massachusetts, 1975).